IEEE Access
Multidisciplinary | Rapid Review | Open Access Journal

Received October 14, 2017, accepted December 20, 2017, date of publication January 18, 2018, date of current version March 12, 2018.

Digital Object Identifier 10.1109/ACCESS.2018.2795028

Scalable Coding and Prioritized Transmission of ECG for Low-Latency Cardiac Monitoring Over Cellular M2M Networks

YONGWOO CHO[1], (Member, IEEE), HEONSHIK SHIN[2], (Member, IEEE), AND KYUNGTAE KANG[3], (Member, IEEE)

[1]Division of Information and Communication Technology, Hanyang University, Ansan 15588, Republic of Korea
[2]Department of Computer Science and Engineering, Seoul National University, Seoul 08826, Republic of Korea
[3]Department of Computer Science and Engineering, Hanyang University, Ansan 15588, Republic of Korea

Corresponding author: Kyungtae Kang (ktkang@hanyang.ac.kr)

This work was supported by the Basic Science Research Program and the Next-Generation Information Computing Development Program, through the National Research Foundation of Korea (NRF) funded by the Ministry of Science and ICT under Grant NRF-2017R1A2B4007970, Grant NRF-2017M3C4A7066207, and Grant NRF-2017M3C4A7083676 and in part by the Research Fund of Hanyang University under Grant HY-2017-N.

ABSTRACT This paper reduces the delay in wireless transmission of electrocardiogram (ECG) data while protecting their essential elements to produce a clinically usable trace. The ECG data are divided into nine layers according to the signal amplitude resolution (6, 8, and 11 bits per sample) and sampling frequency (75, 300, and 2400 Hz). To avoid retransmission, each layer is delivered with a dynamic link adaptation scheme that provides the different levels of error protection in a forward error correction process according to layer importance. This scheme is built on the conservative modulation and coding, as well as on the machine-type communication (MTC) protocol, from LTE-Advanced. Simulations show that our proposed system delivers ECG data that sufficiently support a clinical diagnosis with significantly low latencies (less than 10 ms) under severely erroneous channel conditions.

INDEX TERMS Biomedical telemetry, electrocardiography, Internet of Things, machine-to-machine communications, layered error protection.

I. INTRODUCTION

Recent advances in semiconductor technology have enabled the development of lightweight, portable, and wearable sensor devices that can be used to acquire physical data, whereas wireless technology can now provide continuous connectivity and a high degree of mobility. Moreover, the proliferation of the Internet of Things (IoT) concept, in which numerous heterogeneous mobile sensor devices are connected to remote servers on the Internet, has made it possible for medical sensors to provide telemetry for remote patient monitoring [1], [2]. In this paper, we introduce a cardiac telemetry system, based on cellular IoT technology that achieves low latency without compromising the diagnosis quality [1], [2].

In particular, cellular wireless sensors enable 24-hour, continuous, real-time monitoring of electrocardiographic signals, and can send the patient location to emergency services whenever necessary. This type of service allows a physician to follow a cardiac condition more closely. In addition, emergency medical technicians at the scene can be advised to administer appropriate first-line treatments, including injections of drugs such as epinephrine or lidocaine [3]. However, some medical conditions require a hardwired system to provide immediate display of cardiac data. The American Heart Association (AHA) recently observed that most wireless electrocardiogram (ECG) systems exhibit clinically significant delays that can compromise patient safety [4]. Therefore, the AHA recommends the use of hardwired telemetry systems when ECG data must be available without delay.

Thus, to extend the applicability of wireless ECG, the end-to-end latency of current systems needs to be reduced, but the trace observed by the clinician must still be of sufficient quality for medical diagnosis. The work reported in this paper aims to develop a real-time wireless ECG monitoring system that allows outpatients to be monitored just as closely as patients in a hospital without compromising the diagnosis quality. We achieve this objective by extending our existing

adaptive framework [5]–[7] to incorporate modern cellular machine-to-machine (M2M) technology.

Our work is based upon long-term evolution (LTE) machine-type communication (MTC) technology, which was recently announced by the 3rd Generation Partnership Project (3GPP) to support various M2M scenarios with LTE networks [8]–[10]. This study was initiated with an analysis of the timing aspects for real-time ECG monitoring, from ECG signal acquisition and sampling, to LTE MTC communication procedures. As a result, three major sources of significant nondeterministic delays, largely caused by unnecessary buffers, were identified and eliminated. First, any ECG data encoding steps that require significant buffering were bypassed. Second, a dedicated channel allocation scheme was used in order to yield a substantial reduction in the latency of the packet-scheduling process and to render the remaining latency deterministic. Finally, we eliminated retransmissions performed by an error-control system used by LTE MTC, known as hybrid automatic repeat request (HARQ). The result was a highly reduced end-to-end latency.

Although these modifications reduce the end-to-end processing time, the use of fewer error-control processes inevitably results in a significant increase in the error rate. This problem was addressed in two ways. First, by determining the minimum resolution of ECG data required in different clinical situations, three M2M service profiles were constructed: 1) a mandatory profile for real-time LCD (liquid crystal display) monitors; 2) a standard profile for diagnostic printouts; and 3) a high-precision profile to deliver high-resolution ECG that facilitates detailed feature detection in a trace, such as ventricular late potentials or narrow pacemaker pulses. Then, the ECG data was arranged into layers, a process that by itself incurs no delay and allows the three service profiles to be supported on a unified platform. Second, using both a novel resolution-frequency scalable ECG encoding and a prioritized transmission scheme that identify the most important data layers in the stream to build the three ECG service profiles, the profiles are arranged in levels that reflect their priority. Then, bandwidth is preferentially allocated to the most important layers, providing them with increased error protection.

Finally, we modified the mapping process of the channel quality indicator (CQI) to activate conservative modulation and coding in LTE MTC systems so that the essential part of the ECG stream can be protected against channel errors more effectively. Overall throughput is reduced by conservative modulation and coding, but this provides a usable ECG trace, even under severely erroneous channel conditions, while keeping the overall delay extremely short. Although this scheme appears to overconsume system resources, we found that protecting the essential portions of ECG data significantly reduces signal distortion, especially under severely erroneous channel conditions, as assessed by using a comparison with other schemes to assess the diagnosis quality.

The main contribution of this study is as follows. Although numerous approaches have been proposed for real-time ECG transmission over various wireless technologies, such as wireless body area network (WBAN), wireless personal area network (WPAN), wireless local area network (WLAN), and cellular technology, they are mainly focused on reducing the overall signal distortion and enhancing the quality of the delivered ECG patterns [11]–[13]. To the best of our knowledge, this paper introduces the first delay-optimized approach to ECG transmission, based on LTE MTC, which achieves low end-to-end system latency without sacrificing the signal quality needed for clinical interpretation.

The remainder of this paper is organized as follows. The motivation for this study is briefly described in Section II and some related work is presented in Section III. An analysis of the system latency and signal quality, as well as a delay-optimized M2M ECG signal processing scheme, are presented in Section IV. In Section V, the service architecture used in this study is introduced, and a resolution-frequency scalable coding scheme for ECG data is proposed along with a prioritized MTC channel coding scheme that responds to bandwidth fluctuations and can tolerate severely erroneous channel conditions. In Section VI, our evaluation environment is detailed, and the effectiveness of the proposed prioritized transmission scheme is investigated. Section VII concludes the paper.

II. RESEARCH MOTIVATION

A. CLINICAL REQUIREMENT FOR INSTANTANEOUS MONITORING

According to a recent advisory from the AHA [4], most current wireless ECG systems are likely to exhibit clinically significant delays in displaying continuous ECG data on patient monitoring displays. Given that these delays can threaten the safety of patients, the advisory recommends the use of hardwired systems for instantaneous monitoring situations.

In general, excessive delay in displaying a patient's cardiac status and corresponding ECG patterns can lead to inappropriate medical assessments and incorrect treatment. For example, an adverse event report from the U.S. Food and Drug Administration describes unnecessary defibrillation resulting from a slow cardiac condition assessment [14]. In this case, a physician misjudged a successful electric cardioversion as a failure because the wireless ECG monitor continued to display a series of atrial flutters that had actually occurred several seconds before the shock. In fact, the patient had already been cardioverted to normal status, but the normal sinus rhythm appeared several seconds later, after a second shock was administered. Examples from the AHA advisory [4] of clinical situations that require instantaneous monitoring are given in Table 1.

On a standard LCD display with a refresh rate of 60 Hz, the image is updated approximately every 17 ms. Therefore, our first goal in this study was to design a cellular M2M ECG monitoring system with a latency lower than this single-frame delay to enable low-latency, real-time monitoring for cardiac signals equivalent to a *hardwired level*.

TABLE 1. Clinical situations where instantaneous ECG monitoring is recommended.

Emergency situations
• Resuscitation • Hospital codes • Defibrillation
Assessment of pacemaker function
• Interrogation or reprogramming of implantable pacemakers, defibrillators, and cardiac resynchronization devices • Assessment or reprogramming of temporary pacing devices
Termination or cardioversion of arrhythmias
• Electrical cardioversion • Administration of intravenous adenosine or other short-acting antiarrhythmic drugs
Bedside procedures
• Insertion of central venous or pulmonary artery catheters using jugular or subclavian approach • Insertion of transvenous pacemakers • Carotid sinus massage

III. RELATED WORK

A. ECG MONITORING USING WBANs AND WPANs

Recent surveys on low-power body-area networks [15] suggest that WBANs and WPANs are currently the most common wireless technologies used for medical telemetry in applications such as wearable sensors and smart implants [16], monitoring systems for the elderly [11], and wearable health monitoring systems [17]. In recent studies on WBANs for health monitoring, several low-power WBAN technologies to prolong the network lifetime for intra-, on-, or off-body communications were compared [15]. In addition, a Raspberry Pi implementation of ECG monitoring based on WBAN was recently introduced [18]. Likewise, WPANs have also been used in various recent telemetry studies, including a method of traffic redirection that addresses the coordinator bottleneck issue of real-time ECG monitoring systems [19] and an outdoor monitoring system for the elderly based on ZigBee [20]. Other recent developments using Bluetooth include an algorithm to reduce ECG acquisition noise [21] and a wireless monitoring system based on a field-programmable gate array [22].

WBAN and WPAN systems do not consume much energy because they are based on low-power, short-range radio technology. Thus, these technologies are regarded as the most suitable substitutes to wired communication for patients using ECG monitors in an indoor environment. However, they are not adequate outdoors. Furthermore, the point-to-point connections required by WPAN protocols involve a complicated pairing procedure to initialize, and it must be repeated as a patient moves around. Moreover, the unstable characteristic of the narrow communication bandwidth inhibits the widespread acceptance of WPAN-based systems for critical medical applications.

B. ECG MONITORING USING WLANs

WLANs, which benefit from the popularity of Wi-Fi technology, provide much more stable radio resources for ECG systems than WPANs [23]. Recent developments based on WLAN technology include a multi-parameter vital sign monitor [24], an ECG transmission control system based on the media access control (MAC) layer [25], and a delay-sensitive handoff control scheme [26]. In general, WLAN technologies allow greater system mobility than WPANs and frequent pairing procedures are not required. However, WLAN systems demand more complicated and physically larger hardware. In addition, although WLAN-based systems provide longer range, they have limited utility outdoors or within moving vehicles. Considering these factors related to the different networking technologies, we decided to use cellular networks for our development.

C. ECG MONITORING USING CELLULAR NETWORKS

Systems based on cellular networks are the only truly feasible way to provide emergency functionality, because these networks provide wide coverage with high levels of mobility and reliability [23]. In particular, cellular networks provide more reliability to support mission-critical clinical tasks, as they can ensure a certain level of quality of service (QoS). Recent developments in this area include a novel framework to measure the QoS in mobile health networks [27], a continuous-time, low-pass sigma-delta analog-to-digital converter (ADC) for cellular networks-based ECG monitoring [28], and a service framework for medical-grade, real-time ECG monitoring over cellular networks [7]. However, the higher running cost of cellular systems, more complicated system architectures, and higher power consumption restrict their potential for 24-hour real-time monitoring. In certain situations, seamless ECG data transmission is essential. These situations include telemetry systems for ambulances and monitoring systems for patients at high risk of cardiac failure as the primary applications for LTE MTC in wireless ECG monitoring.

D. EMERGENCE OF LTE MTC

Recently, the 3GPP announced a series of standards [8], [9], [29], [30] to extend LTE of communication services by supporting a range of scenarios for M2M and MTC. The European Telecommunications Standards Institute (ETSI) also published several technical standards [31], [32] to address the increasing demand for various types of M2M applications. Part of the upcoming release of the 3GPP LTE standard is LTE MTC, which is an effort to optimize LTE-Advanced for MTC.

Figure 1 shows an overall system architecture for MTC [10]. MTC is mainly designed to provide an adequate uplink channel for smart metering and smart grids, and thus achieve low-power consumption, small feature size, and a simplified antenna architecture [33]. The 3GPP MTC is expected to supply sufficient reliable wireless channels to cover a wide area, as well as to provide low-cost, small-sized, and energy-efficient mobile hardware [34], [35].

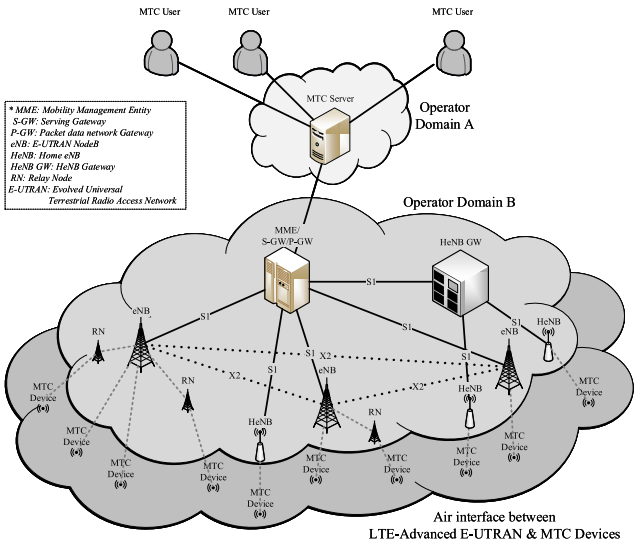

FIGURE 1. MTC system architecture.

The preamble to LTE MTC highlights the many advantages of this approach, including: the reliability, pervasiveness, security, and performance of LTE networks, significantly increased battery life in devices with reduced cost and enhanced coverage, and the ability to benefit from future innovations in its underpinning LTE-Advanced technologies. It is expected that LTE MTC will play a key role in realizing the IoT for various healthcare applications [36], [37].

E. LOW LATENCY REAL-TIME CARDIAC MONITORING OVER LTE MTC

The latency of LTE MTC has been analyzed [38], [39] and evaluated [40] in various previous works. In addition, several studies have been proposed to control or minimize the latency of various signal acquisition systems. For example, a low-power, low-latency processor design to implement a local mean decomposition method for nonlinear and nonstationary ECG signal processing was proposed to reduce the energy cost and execution time for an ECG signal-acquisition chip [41]. A scheme was introduced in [42] to balance the tradeoff between power saving and latency of LTE-Advanced networks by switching the discontinuous reception cycle and inactivity timer based on traffic level. A design scheme for a low-latency, highly reliable wireless communication system to support sensing and control applications was proposed based on the use of reliable broadcasting, semifixed resource allocation, and low-rate coding [43]. However, none of these previous works directly provide an adequate solution for low-latency, real-time cardiac monitoring over LTE MTC.

IV. SYSTEM ANALYSIS AND DESIGN

A. SYSTEM-LEVEL LATENCY ANALYSIS AND A DELAY-ENHANCED M2M ECG SIGNAL PROCESSING SCHEME

With the goal of designing a cellular cardiac monitoring system with lower latency than a single-frame delay of a 60 Hz display, we first analyzed the timing of a real-time ECG monitoring system based on LTE MTC. The end-to-end latency (d_{total}) of that type of system can be expressed as follows:

$$d_{\text{total}} = d_{\text{A}} + d_{\text{D}} + d_{\text{P}} \tag{1}$$

where d_{A}, d_{D}, and d_{P} are the delays in acquisition, delivery, and presentation, respectively.

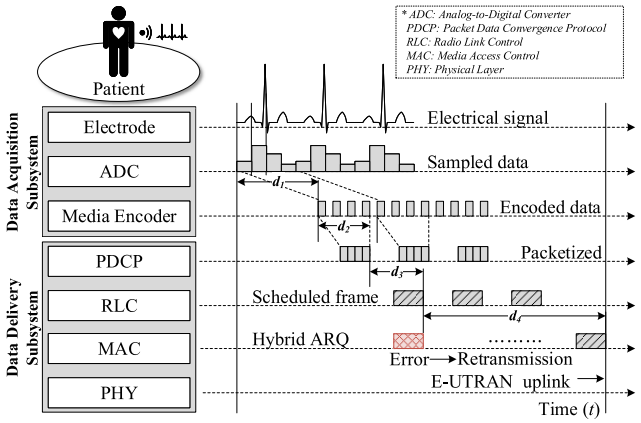

FIGURE 2. System-level latency in real-time ECG transmission over LTE MTC.

As shown in Fig. 2, d_{A} is mainly caused by the media encoder. The LTE system latency is largely responsible for d_{D}, which includes the time required for packetizing, scheduling, and waiting for retransmission. The last delay, d_{P}, depends largely on the characteristics of the display hardware, which are beyond the scope of this study.

For data acquisition, the latency due to media encoding, represented as d_1 in Fig. 2, can be eliminated by omitting the data compression procedure, and the packetizing delay, d_2, can be reduced below 1 ms by using smaller data packets. Data compression is lengthy because data segments are compared within a packet to identify redundancy. If these comparisons are omitted, buffering delays can be substantially shortened. However, without any data compression, the bitrate necessary for the transmission of ECG data could become excessive; therefore, we adopted a layered coding scheme as discussed in Section V-A.

The LTE communication system for data delivery typically has two service planes [30]: a control plane (C-Plane) for signaling and control functions, and a user plane (U-Plane) for the actual delivery function. The C-Plane latency is the time taken by the user equipment (UE) to shift between idle and active states, before initiating the U-Plane communication. It has been estimated that this delay can reach 77.5 ms in standard LTE systems [38]. This high C-Plane latency can be avoided by operating the monitoring system in contention-free mode with pre-allocated system resources. Furthermore, the U-Plane latency can be decreased to 1 or 2 ms by reducing the scheduling delays, represented as d_3 in Fig. 2. This is achieved by using the dedicated service mode of the U-plane with a preset channel bandwidth.

The standard LTE HARQ process involves a long and nondeterministic buffering time, represented as d_4 in Fig. 2, because it can attempt up to three retransmissions whenever necessary [30]. Therefore, we replaced the HARQ retransmission process with a novel physical-layer (PHY) modulation scheme, named prioritized MTC channel coding for error control, which is discussed in Section V-B. This reduces d_4 to the few milliseconds of processing time required for forward error correction.

We have also reduced other delays associated with the encoding, scheduling, and error-control layers by reducing the amount of buffering to achieve total transmission latency below a single-frame delay in 60 Hz displays. Our proposed policy for buffer management involves maintaining each buffer at its lowest level and emptying it at an exactly scheduled timing point. To implement this minimum buffering policy, all the components of our system are synchronized by a system-wide clock signal.

B. GENERALIZED M2M ECG SERVICE PROFILES FOR DIFFERENT CLINICAL SITUATIONS

Medical data, especially vital signals, are usually allocated plentiful computing resources given their clinical significance. Redundant system resources are provided to guarantee appropriate safety margins for medical applications. However, this can have catastrophic consequences when a lack of communication resources fails to deliver full and intact data packets. Hence, it is necessary to carefully consider both the actually required output and the clinical purpose of a system. We now examine the medical information required for an ECG application by considering the specifications of the devices on which a trace is produced.

The actual length, $L_{\mathrm{P}}^{\mathrm{x}}$, in millimeters, along the x axis of an ECG pattern displayed on a presentation device P can be expressed as follows:

$$L_{\mathrm{P}}^{\mathrm{x}} = \frac{N_{\mathrm{P}}^{\mathrm{x}}}{\lambda_{\mathrm{P}}} \tag{2}$$

where λ_{P} is the number of pixels per millimeter on P, and $N_{\mathrm{P}}^{\mathrm{x}}$ is the display width of the device in pixels. If $N_{\mathrm{D}} \geq N_{\mathrm{P}}^{\mathrm{x}}$, where N_{D} is the number of successfully transmitted samples using delivery system D, then every pixel will be fully utilized. The total number, N_{A}, of samples acquired from electrode A is given by

$$N_{\mathrm{A}} = f_{\mathrm{A}} \tau_{\mathrm{A}} \tag{3}$$

where f_{A} is the ECG sampling frequency, and τ_{A} is the data acquisition period. To deliver a sufficient number N_{D} of samples from acquired samples N_{A}, the sampling frequency, f_{D}, of the delivery stream should match or exceed the width of the presentation device in pixels divided by the presentation duration, τ_{P}, which is the timespan for a signal to traverse the screen:

$$f_{\mathrm{D}} \geq \frac{N_{\mathrm{P}}^{\mathrm{x}}}{\tau_{\mathrm{P}}} \tag{4}$$

where

$$\tau_{\mathrm{P}} = \frac{L_{\mathrm{P}}^{\mathrm{x}}}{S_{\mathrm{P}}} \tag{5}$$

and S_{P} is the display speed, which is standardized at 25 mm/s [44]. By substituting (2) and (5) into (4), the following relationship is obtained:

$$f_{\mathrm{D}} \geq S_{\mathrm{P}} \lambda_{\mathrm{P}}. \tag{6}$$

Likewise, the height of the display, $L_{\mathrm{P}}^{\mathrm{y}}$, in millimeters, along the y axis can be expressed as follows:

$$L_{\mathrm{P}}^{\mathrm{y}} = \frac{N_{\mathrm{P}}^{\mathrm{y}}}{\lambda_{\mathrm{P}}} \tag{7}$$

where $N_{\mathrm{P}}^{\mathrm{y}}$ is the display height of the device in pixels. To fully utilize this height, the number of levels, η_{D}, in the discretized signal should at a minimum equal this number of pixels, so that:

$$\eta_{\mathrm{D}} \geq N_{\mathrm{P}}^{\mathrm{y}}. \tag{8}$$

If the peak-to-peak voltage of the signal is V_{PP}, then the presentation density, σ_{P}, in volts per millimeter is given by

$$\sigma_{\mathrm{P}} = \frac{V_{\mathrm{PP}}}{L_{\mathrm{P}}^{\mathrm{y}}}. \tag{9}$$

By substituting (7) and (9) into (8), we obtain

$$\eta_{\mathrm{D}} \geq \frac{V_{\mathrm{PP}} \lambda_{\mathrm{P}}}{\sigma_{\mathrm{P}}}. \tag{10}$$

V_{PP} and σ_{P} are standardized [44] to 10 mV and 100 μV/mm, respectively, but pixel density λ_{P} differs from one device to another. As is shown in Table 2, a standard LCD display for real-time ECG monitoring has 72 ppi (i.e., pixels per inch) or 2.83 pixels/mm. A 300 dpi (i.e., dots per inch) inkjet printer has 11.81 pixels/mm, and a 2400 dpi laser printer has 94.49 pixels/mm.

TABLE 2. Requirements for presentation device type.

	Presentation Device Type		
	72 ppi LCD Panel	300 dpi Inkjet Printer	2400 dpi Laser Printer
λ_{P} (pixels/mm)	2.83	11.81	94.49
$\min(f_{\mathrm{D}})$ (Hz)	70.87	295.28	2362.20
$\min(\eta_{\mathrm{D}})$ (levels)	56.69	236.22	1889.76

TABLE 3. ECG delivery profiles.

	Mandatory	Standard	High Precision
f_{D} (Hz)	75	300	2400
η_{D} (levels)	64 (6 bits)	256 (8 bits)	2048 (11 bits)

Table 3 lists the sampling frequency, f_{D}, and the number of resolution levels, η_{D}, for various devices, and Fig. 3 shows example traces acquired using the standard and mandatory values of f_{D} and η_{D}. The horizontal length of both graphs, which represents 2 s, should be scaled to 5 cm on any display form according to the ECG standard [44].

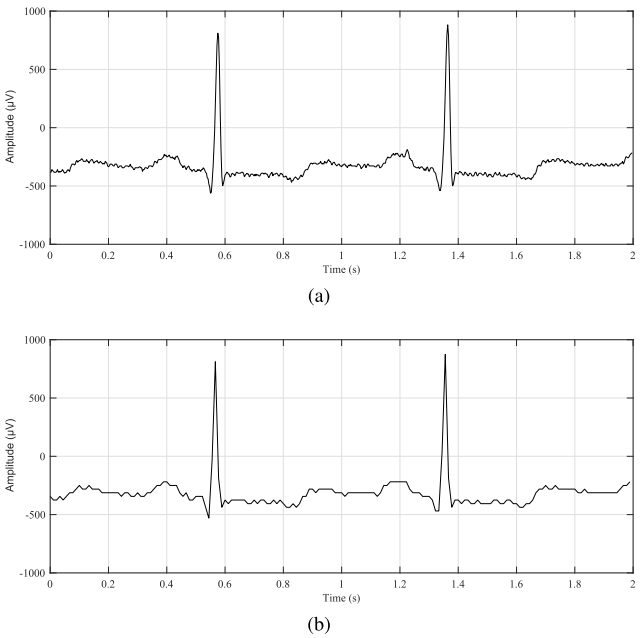

FIGURE 3. Example ECG traces obtained using the (a) standard and (b) mandatory profiles.

The 6 most significant bits of an ECG signal delivered at 75 Hz have been found adequate [45] to make full use of a 72 ppi LCD display, because any extra information does not enhance the diagnostic value of the ECG pattern on that type of device.

Therefore, a 6-bit data stream at 75 Hz is the mandatory profile for real-time ECG monitoring. Moreover, an 8-bit data stream at 300 Hz is the standard for a 300 dpi inkjet printer, and an 11-bit data stream at 2400 Hz for high-resolution traces on a 2400 dpi laser printer. The latter is the highest resolution of any standard profile for ECG data.

V. LOW-LATENCY M2M ECG MONITORING SYSTEM BASED ON LTE MTC

Fig. 4 shows a service scenario for remote ECG monitoring. The patient's heart is monitored by a wireless ECG sensor that consists of multiple electrodes, a wireless transmitter, and a receiver. If the electrical signals from the heart are acquired by N electrodes, and sampled by the ADC at a rate of f (# samples per second) with a sample size of η bits, the transmitter sends the data packets with the following data rate:

$$\mu_{\mathrm{ECG}} = Nf\eta. \tag{11}$$

The digitized ECG stream is packetized for wireless communication and transmitted to remote nodes over a secure LTE MTC channel.

A. RESOLUTION-FREQUENCY SCALABLE ECG CODING FOR PRIORITIZATION

As discussed in Section II, the data acquisition latency can be reduced by omitting data compression. In this section,

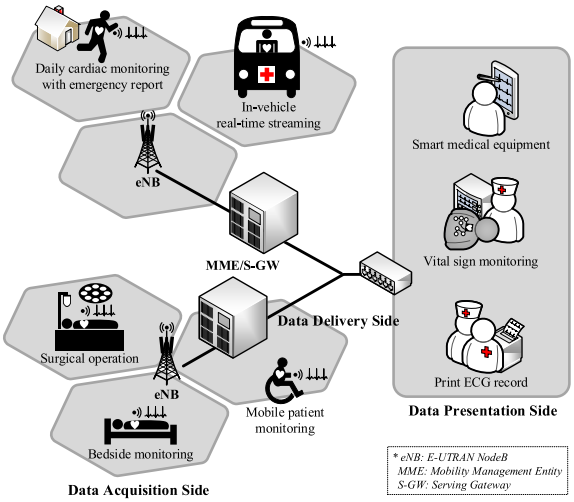

FIGURE 4. Scenario for M2M ECG monitoring based on LTE MTC.

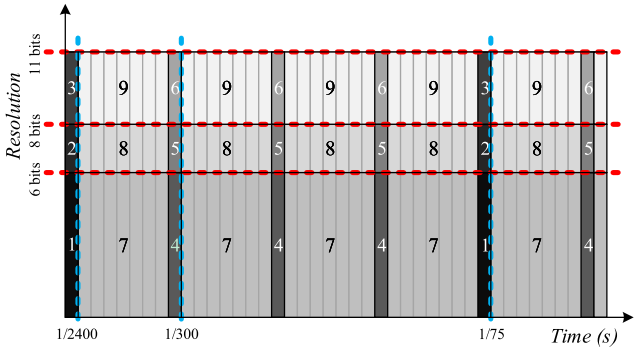

FIGURE 5. Priorities from 1 to 9 assigned to different elements of the ECG data in our transmission scheme, with resolution-frequency scalability.

we introduce an ECG transmission format that is scalable in both the amplitude resolution and sampling frequency domains.

The continuously fluctuating voltage acquired by each ECG electrode is converted to digital data at given amplitude resolution and sampling frequency by an ADC. To make full use of the given bandwidth available for transmission, this study uses a simple dynamic range optimization scheme. The digitized samples are normalized to the range between the minimum and maximum values occurring over a moving time window. Information on these values, which is included in a media packet header, is periodically delivered. Then, the amplitude resolution for transmission of the normalized samples can be scaled by varying the number of transmitted significant bits.

Likewise, the sampling frequency can be scaled by varying the number of transmitted samples. Fig. 5 shows these operations: the minimum amount of data transmitted consists of a 6-bit value every 1/75 s, with the amplitude resolution increasing to 8 and 11 bits as more bandwidth becomes available.

Then low-resolution intermediate values are transmitted every 1/300 s, and their amplitude resolution is increased

in the same manner until 11-bit data are being transmitted every 1/300 s. Furthermore, if the bandwidth permits, more frequent intermediate values are transmitted at 1/2400 s, and their amplitude resolution is also increased. Finally, the maximum bitrate is reached when 2400 samples per second with 11-bit amplitude resolution are being transmitted. Thus, there are nine possible resolution-frequency configurations, corresponding to the numerals 1 to 9 shown on the bars in Fig. 5.

The bitrate, $B(i,j)$, required to deliver the i^{th} sampling frequency level and j^{th} amplitude resolution can be expressed as follows:

$$f_{\text{D}}(0) = 0$$
$$B(i,j) = f_{\text{D}}(i-1)\max(\eta_{\text{D}}) + \{f_{\text{D}}(i) - f_{\text{D}}(i-1)\}\,\eta_{\text{D}}(j) \quad (12)$$

where $f_{\text{D}}(i)$ is the i^{th} sampling frequency, $\eta_{\text{D}}(j)$ is the number of bits for the j^{th} level of amplitude resolution, and $\max(\eta_{\text{D}})$ is the highest number of bits available. The corresponding bitrates are shown in Fig. 6.

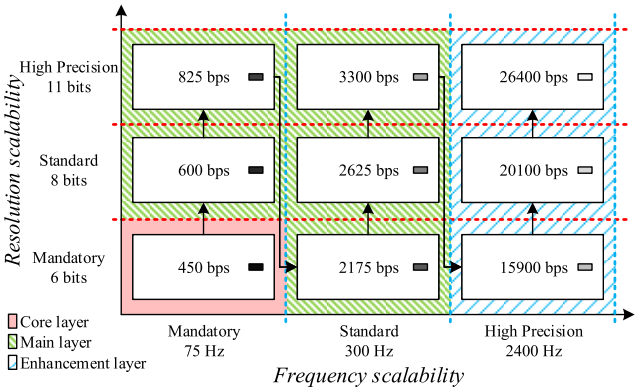

FIGURE 6. Resolution-frequency scalable ECG encoding scheme.

B. CONSERVATIVE CHANNEL CODING TO PROTECT PRIORITIZED LAYERS

LTE systems use adaptive modulation and coding (AMC), in which the modulation scheme and code-rate vary to fit the channel conditions. Higher-order modulation schemes, such as m-ary quadrature amplitude modulation (m-QAM) provide increased spectral efficiency, whereas lower-order schemes such as binary phase-shift keying (BPSK) are more robust under severely erroneous channel conditions. In an MTC system that complies with the LTE-Advanced standard [8], [30], the base station estimates the quality of the uplink channel from the UE, using sounding reference signals of the highest order that the channel quality permits, and assigns the modulation and coding scheme (MCS) that maximizes throughput. There is no attempt to eliminate all transmission errors in this scheme, and the LTE-Advanced standard specifies a residual block error rate (BLER) up to 10%. The residual errors are further reduced by forward error correction, followed by retransmission when necessary, to maximize the overall data rate. For this reason, in the case of standard LTE specification, the lowest-order MCS is limited to quadrature phase-shift keying (QPSK). Table 4 lists the standard mappings from a CQI to an MCS. Fig. 7 shows the BLER and throughput of a simulated MTC uplink using MCSs selected from this table. Further details on this simulation are presented in Section VI.

TABLE 4. Four-bit MCS table.

MCS	Modulation	Code rate ($\times 1024$)	Efficiency(bps/Hz)
0		Out of range	
1	QPSK	78	0.1523
2	QPSK	120	0.2344
3	QPSK	193	0.3770
4	QPSK	308	0.6016
5	QPSK	449	0.8770
6	QPSK	602	1.1758
7	16QAM	378	1.4766
8	16QAM	490	1.9141
9	16QAM	616	2.4063
10	16QAM	466	2.7305
11	16QAM	567	3.3223
12	16QAM	666	3.9023
13	16QAM	772	4.5234
14	16QAM	873	5.1152
15	16QAM	948	5.5547

The LTE-Advanced link adaptation scheme has been modified in various ways by other authors [46]–[49]. We have already stated that our aim is to reduce the end-to-end latency below a single-frame delay of 60 Hz displays. Moreover, we aim to maintain the transmission quality required for ECG data by providing extra protection for higher-priority layers at some cost in overall throughput.

Fig. 6 shows how we segment ECG data into layers to provide resolution-frequency scalability. The *core layer* delivers the amount of data mandated by the AHA advisory, the *main layer* delivers data up to the standard profile level, and the *enhance layer* delivers data quality above the standard profile.

Fig. 8 shows the block diagram of the proposed *conservative channel coding scheme*. As described in Section IV-A, there is no retransmission, and the bandwidth usually reserved for retransmission is reassigned to the more important core and main layers of our scheme.

Because the bandwidth required for the core layer is only 1 or 2% of that required for all layers, BPSK modulation can adequately protect the core-layer data without additional error control.

The data in the main layer is transmitted with a lower MCS for a given CQI, and we call this scheme *conservative CQI mapping*. By reducing the MCS level by one, the received BLER can be reduced by a factor on the order of 10^{-3}. However, the corresponding reductions in bandwidth are relatively modest; for example, changing from MCS #14, which has an efficiency of 5.1152, to MCS #15 with an efficiency of 5.5547, only reduces the available bandwidth by 7.91%. The maximum bandwidth reduction is 37.82% when MCS #3 is substituted with MCS #2.

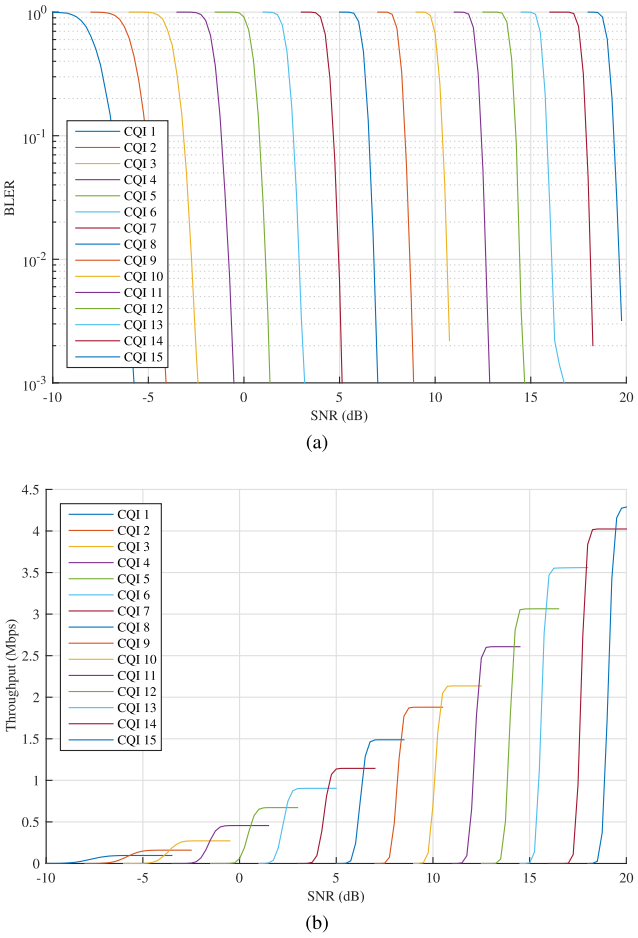

FIGURE 7. Simulation of an MTC with AMC with a bandwidth of 1.4 MHz and a 2.4-GHz carrier frequency compromised by additive white Gaussian noise (AWGN): (a) BLER, and (b) throughput against signal-to-noise ratio (SNR).

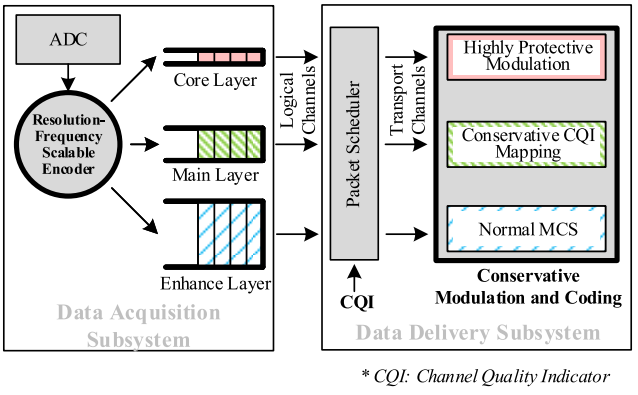

FIGURE 8. Conservative channel coding scheme to protect higher-priority layers.

VI. PERFORMANCE EVALUATION

A. SIMULATION ENVIRONMENT

Simulations were performed on a Vienna LTE-Advanced uplink link-level simulator [50], using ECG data from PhysioBank [51].

TABLE 5. Simulation parameters.

LTE MTC Parameter	Value
Carrier frequency	2.4 GHz
MTC channel bandwidth	1.4 MHz
Antenna configuration	SISO
Channel model	AWGN/WINNER II [52]
Number of UEs	1
UE speed	3 km/h
Maximum number of HARQ retransmissions	
- Standard LTE scheme	3
- Real-time streaming without prioritization	3
- Proposed prioritized transmission scheme	0
Transmission time interval (TTI) duration	1 ms
Number of slots in one subframe	2
Number of subframes in one frame	10

The main parameters of the simulated LTE MTC system are listed in Table 5. The carrier frequency of the simulation platform is 2.4 GHz, and we limited the MTC channel bandwidth to 1.4 MHz to meet the requirements of LTE category-0 for low-power M2M devices [10]. We also limited the antenna configuration to single-input single-output (SISO) mode, according to the recommendation of LTE MTC [9]. Both AWGN and WINNER II (Wireless World Initiative New Radio) channel models [52] were adopted to simulate adequate channel errors. In our simulation, a single-user device moving at a speed of 3 km/h was assumed. The maximum number of HARQ retransmissions for both a standard LTE scheme and real-time streaming scheme without prioritization was set to three, as in the LTE standard, and the retransmission for the proposed prioritized transmission scheme was disabled. In the simulation, the transmission time interval (TTI) was 1 ms, and the number of slots in one sub-frame and the number of sub-frames in one frame were 2 and 10, respectively, as in the LTE standard [10].

We utilized the MIT-BIH (Massachusetts Institute of Technology - Boston's Beth Israel Hospital) arrhythmia database [53] and the ANSI (American National Standards Institute)/AAMI (Association for the Advancement of Medical Instrumentation) EC13 data [54]. The former contains 48, 30-minute excerpts of two-channel ambulatory ECG recordings obtained from 47 patients studied at the BIH Arrhythmia Laboratory between 1975 and 1979. Twenty-three recordings were selected at random from a set of 4,000, 24-hour ambulatory ECG recordings collected from a mixed population of inpatients (approximately 60%) and outpatients (approximately 40%) at BIH. The remaining 25 recordings were selected from the same set to include less common but clinically significant arrhythmias (such as complex ventricular, junctional, and supraventricular arrhythmias and conduction abnormalities) that would not be represented well in a small random sample. The recordings were digitized at 360 samples per second per channel, with 11 bit resolution, over a 10 mV range, as listed in Table 6.

The 10 short recordings of ANSI/AAMI EC13 test waveforms available in PhysioBank are specified by the current American National Standard for testing various devices that

TABLE 6. Signal parameters of test ECG patterns.

ECG Database	f_A (Hz)	η_A (bits)	N_A
MIT-BIH arrhythmia database [53]	360	11	2
ANSI/AAMI EC13 [54]	720	12	1

measure heart rate, each of which contains one ECG signal sampled at 720 Hz with 12-bit resolution. EC13 also specifies the use of specific synthesized waveforms that can be created using the ECG waveform generator available in PhysioToolkit.

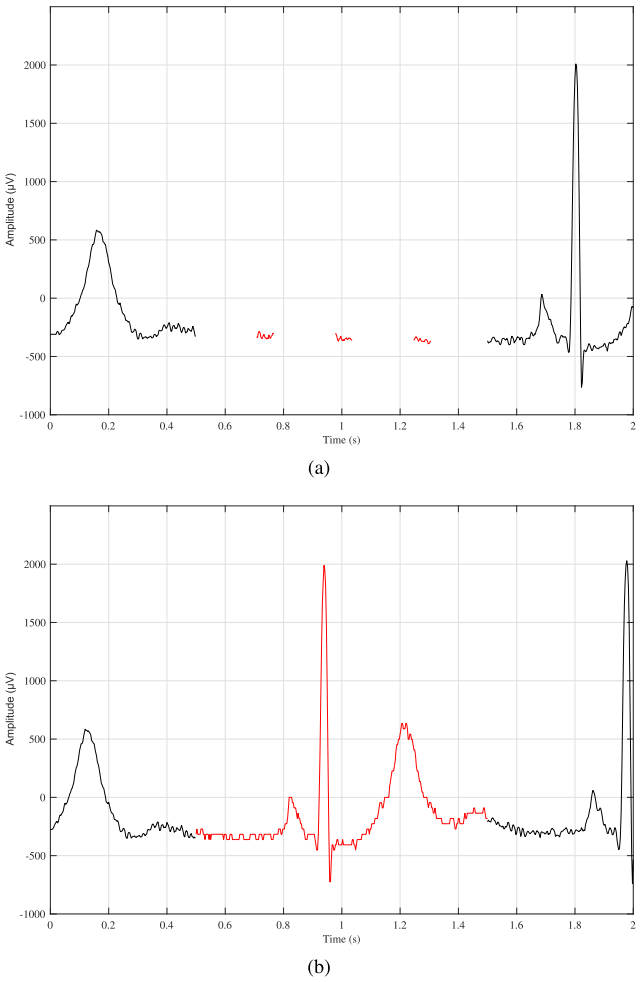

FIGURE 9. Differences in delivered ECG patterns in burst erroneous channel condition: (a) buffering delay in a standard LTE scheme with reduced buffer and (b) timely delivered pattern with subtle quality decline using the proposed prioritized transmission scheme.

B. SIMULATION RESULTS

Fig. 9 and Fig. 10 compare the differences between the proposed prioritized transmission scheme and both a standard LTE scheme with reduced buffer and a real-time streaming system without prioritization under considerably erroneous channel conditions (i.e., packet error rate (PER) 5%), respectively. First, the reduced-buffer scheme requires frequent

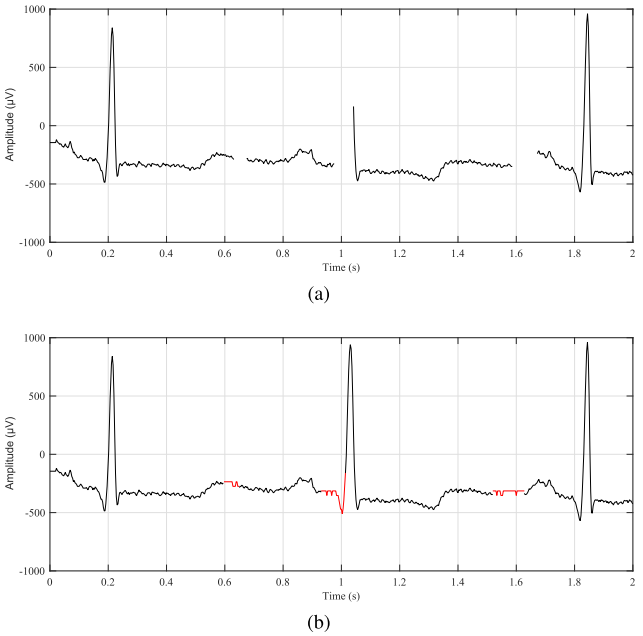

FIGURE 10. Effect of severely erroneous channel condition on the delivered ECG trace: (a) signal skipping in real-time streaming without prioritization, and (b) subtle quality degradation in the proposed scheme, which ensures trace continuity.

buffering delays that distort the ECG pattern. Then, although the real-time streaming system is capable of reducing the communication latency, it cannot handle accidental episodes of transient errors that cause signal skipping. However, with the help of highly protective modulation, the proposed system can successfully deliver the mandatory part of the ECG signal within 10 ms. Therefore, our scheme not only satisfies the timing requirement for instantaneous monitoring purposes but also ensures the basic readability of the transmitted ECG trace.

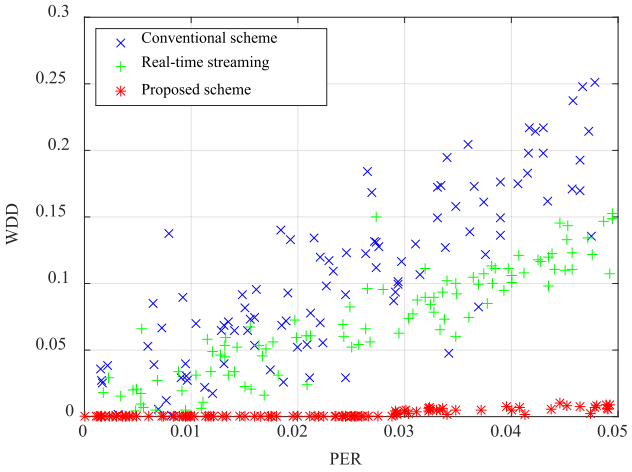

FIGURE 11. WDD of the three transmission schemes.

Fig. 11 compares the weighted diagnostic distortion (WDD), which evaluates the diagnostic features of corrupted ECG signals [55], [56] between the conventional best-effort

standard LTE scheme, real-time streaming without prioritization, and our proposed prioritized transmission system. The proposed scheme outperforms the two other schemes because its protected portion of mandatory ECG data provides a sufficient level of clinically meaningful features, whereas the random unrecoverable damage of the other schemes leads to substantial overall quality degradation.

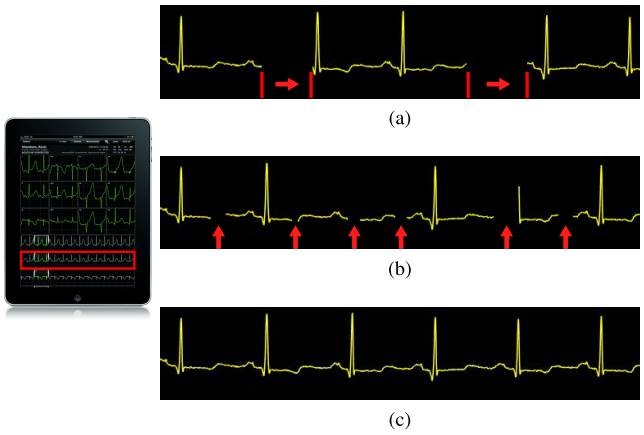

FIGURE 12. ECG patterns rendered on a test monitoring system (PER of 5%). (a) A trace obtained using a standard LTE uplink shows the buffering delay effects. (b) A trace obtained by real-time streaming without prioritization exhibits signal skipping. (c) The proposed prioritized transmission scheme produces a usable trace.

Fig. 12 shows a simulation of the visual effect on the displayed pattern for a commonly available multi-parameter vital monitoring system. As shown in the figure, the ECG trace rendered by the proposed scheme and displayed on the LCD of a typical tablet-based monitor appears adequate for medical purposes, despite the severely erroneous channel conditions. In contrast, both the pattern skipping of the real-time stream system without prioritization and the buffering delay of the conventional best-effort standard LTE scheme appear to seriously disrupt the clinical usability of the transmitted ECG signals.

VII. CONCLUSION

We introduced a low-latency communication system for continuous electrocardiographic monitoring. We analyzed the latency of a real-time ECG monitoring system based on LTE MTC and proposed a modified transmission scheme with a reduced delay to meet clinical requirements. The scheme segments ECG data into layers in both amplitude resolution and sampling frequency, and provides enhanced protection by adopting conservative channel coding for prioritized data layers that are crucial to the clinical interpretation of the signal. Even under severely erroneous channel conditions, simulation results suggest that the end-to-end latency of the proposed system is maintained below 10 ms, which is less than a single-frame delay of a 60 Hz display. Furthermore, any distortion of the ECG trace appears to be less likely to affect diagnosis by using our scheme.

It is clear that no scheme of this type is entirely proven until it has been tried in practice. However, the implementation and testing of medical systems is fraught with difficulties, from patient confidentiality to legal concerns, and cannot reasonably be undertaken until there is as much confidence as possible in the techniques and associated parameters being deployed. It is this confidence that we aim to build in this study through simulations based on offline data.

ACKNOWLEDGMENT

Preliminary version of this paper was presented at the ACM Annual International Conference on Mobile Computing and Networking, Snowbird, UT, USA.

REFERENCES

[1] G. Hindricks and N. Varma, "Remote monitoring and heart failure: Monitoring parameters, technology, and workflow," *Eur. Heart J.*, vol. 37, no. 41, pp. 3164–3166, Jul. 2016.

[2] R. Dierckx, P. Pellicori, J. G. F. Cleland, and A. L. Clark, "Telemonitoring in heart failure: Big brother watching over you," *Heart Faiure Rev.*, vol. 20, no. 1, pp. 107–116, Jan. 2015.

[3] B. J. Drew *et al.*, "Practice standards for electrocardiographic monitoring in hospital settings," *Circulation*, vol. 110, no. 17, pp. 2721–2746, Oct. 2004.

[4] M. P. Turakhia *et al.*, "Latency of ECG displays of hospital telemetry systems," *Circulation*, vol. 126, no. 13, pp. 1665–1669, Sep. 2012.

[5] K. Kang, M.-Y. Nam, and L. Sha, "Model-based analysis of wireless system architectures for real-time applications," *IEEE Trans. Mobile Comput.*, vol. 12, no. 2, pp. 219–232, Feb. 2013.

[6] Y. Cho, J. Ryu, J. Park, J. Lee, H. Shin, and K. Kang, "Scalable ECG transmission to improve the diagnosability of remote patient," in *Proc. IEEE Int. Conf. Consum. Electron.*, Las Vegas, NV, USA, Jan. 2013, pp. 268–269.

[7] K. Kang, Q. Wang, J. Hur, K. J. Park, and L. Sha, "Medical-grade quality of service for real-time mobile healthcare," *Computer*, vol. 48, no. 2, pp. 41–49, Feb. 2015.

[8] *System Improvements for MTC*, document TR 23.888 v11.0.0, 3rd Generation Partnership Project, Valbonne, France, Sep. 2012.

[9] *Study on Provision of Low-Cost Machine-Type Communications (MTC) User Equipments (UEs) Based on LTE (Release 12)*, document TR 36.888 v12.0.0, 3rd Generation Partnership Project, Valbonne, France, Jun. 2013.

[10] *Service Requirements for Machine-Type Communications (MTC) (Release 14)*, document TS 22.368 v14.0.0, Valbonne, France, Mar. 2017.

[11] M. M. Baig, H. Gholamhosseini, and M. J. Connolly, "A comprehensive survey of wearable and wireless ECG monitoring systems for older adults," *Med. Biol. Eng. Comput.*, vol. 51, no. 5, pp. 485–495, 2013.

[12] C.-F. Lin, "Mobile telemedicine: A survey study," *J. Med. Syst.*, vol. 36, no. 2, pp. 511–520, Apr. 2012.

[13] V. Custodio, F. Herrera, G. López, and J. Moreno, "A review on architectures and communications technologies for wearable health-monitoring systems," *Sensors*, vol. 12, no. 10, pp. 13907–13946, Oct. 2012.

[14] "MAUDE adverse event report: Philips healthcare: Philips cardiac monitor: Telemetry monitor," U.S. Food and Drug Admin., Silver Spring, MD, USA, Tech. Rep. 1252144, Jan. 2008. [Online]. Available: https://www.accessdata.fda.gov/scripts/cdrh/cfdocs/cfMAUDE/Detail.CFM?MDRFOI__ID=1252144

[15] M. Ghamari, H. Arora, R. S. Sherratt, and W. Harwin, "Comparison of low-power wireless communication technologies for wearable health-monitoring applications," in *Proc. Int. Conf. Comput., Commun., Control Technol.*, Kuching, Malaysia, Apr. 2015, pp. 1–6.

[16] J. Andreu-Perez, D. R. Leff, H. M. D. Ip, and G.-Z. Yang, "From wearable sensors to smart implants—Toward pervasive and personalized healthcare," *IEEE Trans. Biomed. Eng.*, vol. 62, no. 12, pp. 2750–2762, Dec. 2015.

[17] A. Pantelopoulos and N. G. Bourbakis, "A survey on wearable sensor-based systems for health monitoring and prognosis," *IEEE Trans. Syst., Man, Cybern. C, Appl. Rev.*, vol. 40, no. 1, pp. 1–12, Jan. 2010.

[18] M. U. H. A. Rasyid, A. A. Pranata, B. H. Lee, F. A. Saputra, and A. Sudarsono, "Portable electrocardiogram sensor monitoring system based on body area network," in *Proc. IEEE Int. Conf. Consum. Electron. Taiwan*, Nantou, Taiwan, May 2016, pp. 1–2.

[19] C. H. Tseng, "Coordinator traffic diffusion for data-intensive Zigbee transmission in real-time electrocardiography monitoring," *IEEE Trans. Biomed. Eng.*, vol. 60, no. 12, pp. 3340–3346, Dec. 2013.

[20] J. Wang, T. Fujiwara, T. Kato, and D. Anzai, "Wearable ECG based on impulse-radio-type human body communication," *IEEE Trans. Biomed. Eng.*, vol. 63, no. 9, pp. 1887–1894, Sep. 2016.

[21] U. T. Pandya and U. B. Desai, "A novel algorithm for Bluetooth ECG," *IEEE Trans. Biomed. Eng.*, vol. 59, no. 11, pp. 3148–3154, Nov. 2012.

[22] K.-C. Lin and W.-C. Fang, "A highly integrated hardware design implemented on FPGA for a wireless healthcare monitoring system," in *Proc. IEEE Int. Conf. Consum. Electron. Taiwan*, Taipei, Taiwan, May 2014, pp. 187–188.

[23] E. Kartsakli *et al.*, "A survey on M2M systems for mHealth: A wireless communications perspective," *Sensors*, vol. 14, no. 10, pp. 18009–18052, Sep. 2014.

[24] A. Rizal, V. Suryani, J. Jondri, and S. Hadiyoso, "Development of wireless Patient's vital sign monitor using wireless LAN (IEEE. 802.11. B/G) protocol," *Int. J. Elect. Comput. Eng.*, vol. 4, no. 6, pp. 893–901, Dec. 2014.

[25] J. Park and K. Kang, "Predictable and reliable ECG monitoring over IEEE 802.11 WLANs within a hospital," *Telemed. e-Health*, vol. 20, no. 9, pp. 875–882, Aug. 2014.

[26] Z. Xiaodan and J. Tigang, "A novel cloud based hospital health care service network framework with delay sensitive handoff guarantee," in *Proc. Int. Conf. Service Syst. Service Manage.*, Kunming, China, Jun. 2016, pp. 1–5.

[27] S. Adibi, "Biomedical sensing analyzer (BSA) for mobile-health (mHealth)-LTE," *IEEE J. Biomed. Health Inform.*, vol. 18, no. 1, pp. 345–351, Jan. 2014.

[28] W. C. Lai, J. F. Huang, W. C. Chen, and F. T. Kao, "A continuous-time low-pass sigma-delta ADC chip design for LTE communication application and bio-signal acquisitions," in *Proc. Int. Congr. Image Signal Process.*, Dalian, China, Oct. 2014, pp. 1079–1084.

[29] *Study Facilitating M2M Communication in 3GPP Systems*, document TR 22.868 v8.0.0, 3rd Generation Partnership Project, Valbonne, France, Mar. 2007.

[30] *Evolved Universal Terrestrial Radio Access (E-UTRA): Physical Channels and Modulation (Release 14)*, document TS 36.211 v14.2.0, 3rd Generation Partnership Project, Valbonne, France, Mar. 2017.

[31] *M2M Service Requirements*, document TS 102.689 v2.1.1, European Telecommunications Standards Institute, Valbonne, France, Jun. 2013.

[32] *M2M Functional Architecture*, document TS 102.690 v1.1.1, European Telecommunications Standards Institute, Valbonne, France, Oct. 2011.

[33] D. Niyato, L. Xiao, and P. Wang, "Machine-to-machine communications for home energy management system in smart grid," *IEEE Commun. Mag.*, vol. 49, no. 4, pp. 53–59, Apr. 2011.

[34] B. Ekelund, "The technical challenges of the future generations of telecommunication technologies (LTE/4G)," in *Proc. Int. Symp. VLSI Technol. Syst. Appl.*, Hsinchu, Taiwan, Apr. 2010, pp. 6–8.

[35] K. Zheng, F. Hu, W. Wang, W. Xiang, and M. Dohler, "Radio resource allocation in LTE-advanced cellular networks with M2M communications," *IEEE Commun. Mag.*, vol. 50, no. 7, pp. 184–192, Jul. 2012.

[36] G. Wu, S. Talwar, K. Johnsson, N. Himayat, and K. D. Johnson, "M2M: From mobile to embedded Internet," *IEEE Commun. Mag.*, vol. 49, no. 4, pp. 36–43, Apr. 2011.

[37] P. K. Verma *et al.*, "Machine-to-machine (M2M) communications: A survey," *J. Netw. Comput. Appl.*, vol. 66, pp. 83–105, May 2016.

[38] N. Nikaein and S. Krea, "Latency for real-time machine-to-machine communication in LTE-based system architecture," in *Proc. Eur. Wireless Conf.*, Vienna, Austria, Apr. 2011, pp. 1–6.

[39] A. Rusan and R. Vasiu, "Assessment of packet latency on the 4G LTE S1-U interface: Impact on end-user throughput," in *Proc. Int. Conf. Softw., Telecommun. Comput. Netw.*, Split, Croatia, Sep. 2015, pp. 305–309.

[40] M. P. Wylie-Green and T. Svensson, "Throughput, capacity, handover and latency performance in a 3GPP LTE FDD field trial," in *Proc. IEEE Global Telecommun. Conf.*, Miami, FL, USA, Dec. 2010, pp. 1–6.

[41] H.-C. Hsueh and S.-Y. Chien, "A low-power low-latency processor for real-time on-line local mean decomposition," in *Proc. IEEE Int. Conf. Electron Devices Solid-State Circuits*, Singapore, Jun. 2015, pp. 205–208.

[42] A. T. Koc, S. C. Jha, R. Vannithamby, and M. Torlak, "Device power saving and latency optimization in LTE-A networks through DRX configuration," *IEEE Trans. Wireless Commun.*, vol. 13, no. 5, pp. 2614–2625, May 2014.

[43] M. Weiner, M. Jorgovanovic, A. Sahai, and B. Nikolić, "Design of a low-latency, high-reliability wireless communication system for control applications," in *Proc. IEEE Int. Conf. Commun.*, Sydney, NSW, Australia, Jun. 2014, pp. 3829–3835.

[44] T. B. Garcia, *12-Lead ECG: The Art of Interpretation*. Burlington, MA, USA: Jones & Bartlett, 2013.

[45] D. W. E. Schobben, R. A. Beuker, and W. Oomen, "Dither and data compression," *IEEE Trans. Signal Process.*, vol. 45, no. 8, pp. 2097–2101, Aug. 1997.

[46] P. Li, H. Zhang, B. Zhao, and S. Rangarajan, "Scalable video multicast with adaptive modulation and coding in broadband wireless data systems," *IEEE/ACM Trans. Netw.*, vol. 20, no. 1, pp. 57–68, Feb. 2012.

[47] G. Araniti, M. Condoluci, L. Militano, and A. Iera, "Adaptive resource allocation to multicast services in LTE systems," *IEEE Trans. Broadcast.*, vol. 59, no. 4, pp. 658–664, Dec. 2013.

[48] J. Meng and E. H. Yang, "Constellation and rate selection in adaptive modulation and coding based on finite blocklength analysis and its application to LTE," *IEEE Trans. Wireless Commun.*, vol. 13, no. 10, pp. 5496–5508, Oct. 2014.

[49] D. J. Dechene and A. Shami, "Energy-aware resource allocation strategies for LTE uplink with synchronous HARQ constraints," *IEEE Trans. Mobile Comput.*, vol. 13, no. 2, pp. 422–433, Feb. 2014.

[50] M. Rupp, S. Schwarz, and M. Taranetz, *The Vienna LTE-Advanced Simulators: Up and Downlink, Link and System Level Simulation*. New York, NY, USA: Springer, 2016.

[51] A. L. Goldberger *et al.*, "PhysioBank, PhysioToolkit, and PhysioNet: Components of a new research resource for complex physiologic signals," *Circulation*, vol. 101, no. 23, pp. e215–e220, Jun. 2000.

[52] L. Hentilä, P. Kyösti, M. Käske, M. Narandzic, and M. Alatossava. (Dec. 2007). MATLAB Implementation of the WINNER Phase II Channel Model ver1.1. [Online]. Available: http://projects.celtic-initiative.org/winner+/phase_2_model.html

[53] G. B. Moody and R. G. Mark, "The impact of the MIT-BIH arrhythmia database," *IEEE Eng. Med. Biol. Mag.*, vol. 20, no. 3, pp. 45–50, May/Jun. 2001.

[54] *Cardiac Monitors, Heart Rate Meters, and Alarms*, American National Standard ANSI/AAMI EC13:2002, American National Standards Institute, New York, NY, USA and Association for the Advancement of Medical Instrumentation, Arlington, VA, USA, 2002.

[55] Y. Zigel, A. Cohen, and A. Katz, "The weighted diagnostic distortion (WDD) measure for ECG signal compression," *IEEE Trans. Biomed. Eng.*, vol. 47, no. 11, pp. 1422–1430, Nov. 2000.

[56] K.-J. Park, H.-H. Lee, S. Choi, and K. Kang, "Design of a medical-grade QoS metric for wireless environments," *Trans. Emerg. Telecommun. Technol.*, vol. 27, no. 8, pp. 1022–1029, Aug. 2016.

YONGWOO CHO (S'06–M'17) received the Premedical degree from the University of Ulsan College of Medicine in 1997, the B.S. degree in computer science from Korea National Open University in 2004, and the M.S. and Ph.D. degrees in electrical engineering and computer science from Seoul National University in 2006 and 2017, respectively.

He was with Dooin Corporation and KT Music as a Research Engineer and a General Manager of the Strategic Planning Division. In 2017, he joined the Division of Information and Communication Technology, Hanyang University, Korea, where he is currently an Assistant Professor. His research interest generally lies in cyber-physical systems, mobile computing, health care, and big data. He is a member of the ACM and the IEEE Computer Society.

HEONSHIK SHIN (M'88) received the B.S. degree in applied physics from Seoul National University, Korea, in 1973, and the Ph.D. degree in computer engineering from The University of Texas at Austin in 1985.

He is currently a Professor Emeritus with the Department of Computer Science and Engineering, Seoul National University, Korea. His research interests include mobile computing, distributed systems, real-time systems, fault-tolerant computing, and data storage. He is a member of the ACM and the IEEE Computer Society.

KYUNGTAE KANG (S'05–M'06) received the B.S. degree in computer science and engineering and the M.S. and Ph.D. degrees in electrical engineering and computer science from Seoul National University, Korea, in 1999, 2001, and 2007, respectively.

From 2008 to 2010, he was a Post-Doctoral Research Associate with the University of Illinois at Urbana–Champaign. In 2011, he joined the Department of Computer Science and Engineering, Hanyang University, Korea, where he is currently an Associate Professor. His research interests lie primarily in systems, including operating systems, wireless systems, distributed systems, and real-time embedded systems. His recent research interest is in the interdisciplinary area of cyber-physical systems. He is a member of the ACM and the IEEE Computer Society.